

Two components of transmitter release at a central synapse

YUKIKO GODA* AND CHARLES F. STEVENS†

*Molecular Neurobiology Laboratory and †Howard Hughes Medical Institute, The Salk Institute, 10010 North Torrey Pines Road, La Jolla, CA 92037

Contributed by Charles F. Stevens, September 7, 1994

ABSTRACT After the arrival of a presynaptic nerve impulse at an excitatory synapse in hippocampal neurons, the rate of neurotransmitter release increases rapidly and then returns to low levels with a biphasic decay. The two kinetically distinct components are differentially affected when Sr²⁺ is substituted for Ca²⁺ ions. Our findings are comparable to those of the classical studies for the frog neuromuscular junction, and thus the basic aspects of Ca²⁺-activated transmitter release machinery appear to be conserved in central synapses. The method we have used, in addition, permits us to estimate the average neurotransmitter release rate for a single bouton. The observation of differential Ca²⁺/Sr²⁺ sensitivity is consistent with a release mechanism mediated by two Ca²⁺ sensors with distinct Ca²⁺ affinities: the low-affinity Ca²⁺ sensor facilitates the fast synchronous phase of release, whereas the high-affinity sensor sustains the slow asynchronous phase of release.

Classical electrophysiological studies of synaptic transmission, most notably at the frog neuromuscular junction, have demonstrated the possibility of multiple mechanisms of Ca²⁺-dependent transmitter release based on distinct phases of exocytotic rates and pharmacology: the rate of transmitter release after the initial rapid rise appeared to decay biphasically (1), and the two components of release exhibited differential sensitivity toward the external concentrations of Ca²⁺, Mg²⁺, and Sr²⁺ (2, 3). In another study, the increase in the size of evoked transmitter release elicited by a repetitive stimulation decayed with four kinetically distinct components that again showed differential sensitivity toward various divalent cations (4).

Although fundamental aspects of synaptic transmission in neuromuscular junctions are thought to be conserved in central synapses, some important differences between peripheral and central transmission have been recognized in recent studies (5). We have therefore initiated a characterization of the stimulus-evoked transmitter release in a central synapse, using cultured hippocampal neurons as a model system.

MATERIALS AND METHODS

Cell Culture. Dissociated hippocampal neurons were prepared from embryonic day 15–17 C57BL/6 mice (Harlan–Sprague–Dawley) and cultured as described (6–8). Cell cultures were used for recording 8–13 days after plating.

Electrophysiology. Dual whole-cell patch clamp recordings from paired cells were carried out as described (8). Concentrations of external CaCl₂, SrCl₂, and MgCl₂ were varied as indicated. Microperfusion experiments were done as outlined (8), and boutons were visualized by synapsin I immunofluorescence (9).

RESULTS

To examine transmitter release in central neurons, we monitored synaptic transmission between pairs of hippocampal

pyramidal neurons in primary culture. Synaptic responses measured from a pair of neurons were averaged across stimulation trials and then time averaged over 10-ms bins to create histograms that estimate the quantal release rate as function of time (see *Appendix*). Such histograms reveal at least two kinetically distinct components of neurotransmitter release, which can be described by the following empirical double-exponential equation:

$$\text{release}(t) = Ae^{-at} + Be^{-bt} + C$$

(Fig. 1 *Upper* and Table 1). The fast component (that is, the first exponent) decays more rapidly than the limit of resolution of our method—a decay time constant of 5–10 ms set by the decay of the response to a single quantum of neurotransmitter—and the second exponent exhibits an exponential decay with a time constant in the range of 100–200 ms. Although the method we have used (see *Appendix*) does not permit an estimation of the time constant for the rapid decay, we can accurately determine the number of quanta that are “synchronously” released. In addition the slow component of release is distinct from the slow phase of the synaptic current mediated by the *N*-methyl-D-aspartate subclass of glutamate receptors in hippocampal neurons (10). Control experiments carried out in the presence of 50 μM D-2-amino-5-phosphonovaleric acid to block *N*-methyl-D-aspartate receptors exhibited the typical biphasic decay of responses due to synchronous and asynchronous releases, and the magnitude of the slow component was not significantly different in the presence of D-2-amino-5-phosphonovaleric acid (in 0.5 mM Mg²⁺/10 mM Ca²⁺; data not shown).

We sought to test whether Sr²⁺, an ion that most efficiently substitutes for Ca²⁺ in promoting transmitter release, would mediate transmission at a central synapse and, furthermore, to test whether Sr²⁺ has differential effects on the two components of synaptic response described above.

Sr²⁺ does indeed support synaptic transmission in hippocampal neurons but at much reduced efficiency; Sr²⁺ replacement greatly reduced the fast synchronous component of synaptic response (Figs. 1 and 2), but the slow, asynchronous release component remained intact and in general was greatly facilitated by Sr²⁺ substitution (Figs. 1 and 2; Tables 1 and 2). Thus differential effects of Sr²⁺ ion substitution on multiple components of release, characteristic of frog neuromuscular junctions, for example, are also observed at central synapses, and the mechanisms of Ca²⁺-mediated release appear to be conserved.

The Ca²⁺ dependence of transmitter release has been described by an empirical equation proposed by Dodge and Rahamimoff (11). We find that, in various extracellular Ca²⁺ or Sr²⁺ ion concentrations, both components of release can be well fitted by a Dodge–Rahamimoff equation with a cooperativity parameter of $n = 4$ (Fig. 3). Thus Sr²⁺ must adequately bind to the transmitter release machinery, and the efficacy of the subsequent release process must be altered differentially between the fast and the slow components.

The publication costs of this article were defrayed in part by page charge payment. This article must therefore be hereby marked “advertisement” in accordance with 18 U.S.C. §1734 solely to indicate this fact.

Abbreviation: mEPSC, miniature excitatory postsynaptic current.

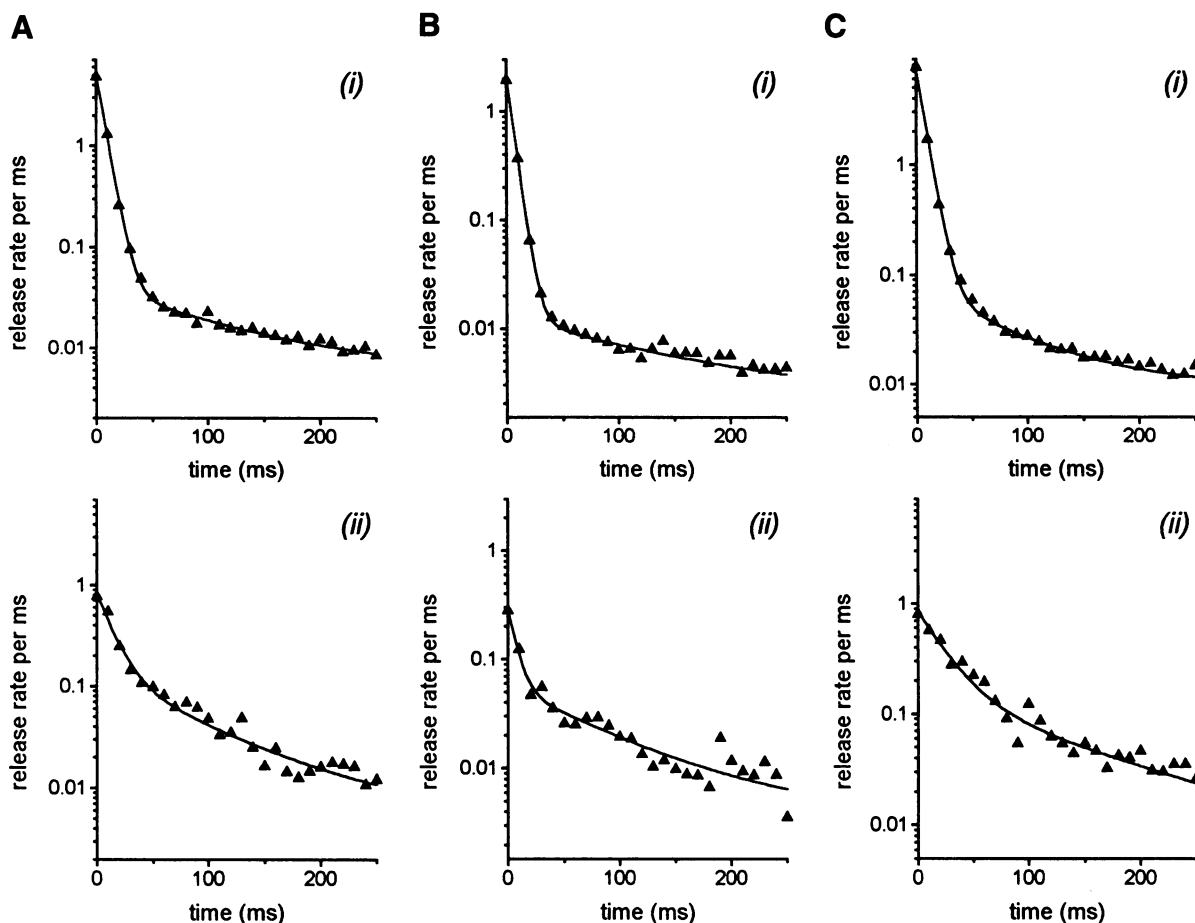


FIG. 1. Synaptic responses display two components of decay. Recordings from three pairs of neurons (9–10 days old) in 2 mM Mg^{2+} /3 mM X (A), 2 mM Mg^{2+} /5 mM X (B), and 0.5 mM Mg^{2+} /10 mM X (C) are shown. Average synaptic responses ($n = 20$) in $X = Ca^{2+}$ in (i) and in $X = Sr^{2+}$ in (ii) from each pair of cells were time averaged over 10-ms bins and are expressed as the total number of quanta released per millisecond (release rate) as a function of time. The number of quanta released was estimated from the average charge of a miniature excitatory postsynaptic current (mEPSC), a single quantum, which is ≈ 100 fC. The rate measured in this way is proportional to the actual rate of quantal release (see *Appendix*); only relative rates are meaningful because the number of contributing synapses is unknown. The points were fitted to the double-exponential equation described in the text. The fast component is defined as the average number of quanta transferred in the initial 20 ms (the first two bins of the release rate histogram) of synaptic response and is expressed as F in Tables 1 and 2. The fast component defined as such is more realistic than the coefficient A , since at this time we cannot accurately determine the time course of the slow component when it overlaps with the Ca^{2+} transient in the presynaptic terminal. In general, F gives a conservative estimate (an upper limit) of the synchronous release than the extrapolated value of A (see Table 1). For example, cumulative distributions of F and A determined from synaptic responses in 20 pairs of cells in 0.5 mM Mg^{2+} /10 mM Ca^{2+} give 1.8 ± 0.5 (mean \pm SEM; SD = 1.9) quanta per ms and 2.6 ± 0.6 (\pm SEM; SD = 2.8) quanta per ms, respectively (data not shown). The final term C , a constant in the above equation, represents the basal rate of mEPSCs. Nevertheless, the value of C is subject to a relatively large error associated with determining the baseline for integrating synaptic currents.

To describe the properties of synaptic transmission at individual synapses, we have characterized transmitter release from a small population of identified boutons to estimate the average quantal release rate per single bouton. Selective activation of a discrete set of boutons was made

possible by locally microperfusing a solution containing high Ca^{2+} and low Mg^{2+} concentrations, which limited synaptic activation to the perfused area; the rest of the cells were bathed in solution with low Ca^{2+} and high Mg^{2+} concentrations, which prevented synaptic currents. The microperfused

Table 1. Parameters used to fit the double-exponential equation displayed in Fig. 1

	X	A , n/ms	a , ms^{-1}	B , n/ms	b , ms^{-1}	C , n/ms	F^* , n/ms
2 mM Mg^{2+} /3 mM X (Fig. 1A)							
(i)	Ca^{2+}	4.80	0.15	0.035	0.01	0.006	3.05
(ii)	Sr^{2+}	0.68	0.07	0.13	0.013	0.006	0.065
2 mM Mg^{2+} /5 mM X (Fig. 1B)							
(i)	Ca^{2+}	1.97	0.18	0.011	0.008	0.0023	1.16
(ii)	Sr^{2+}	0.23	0.14	0.051	0.012	0.004	0.2
0.5 mM Mg^{2+} /10 mM X (Fig. 1C)							
(i)	Ca^{2+}	6.80	0.14	0.07	0.014	0.0096	4.64
(ii)	Sr^{2+}	0.69	0.04	0.15	0.008	0.0037	0.68

n , Estimated number of quantal release (see Fig. 1 legend).

*Fast component (defined in Fig. 1 legend).

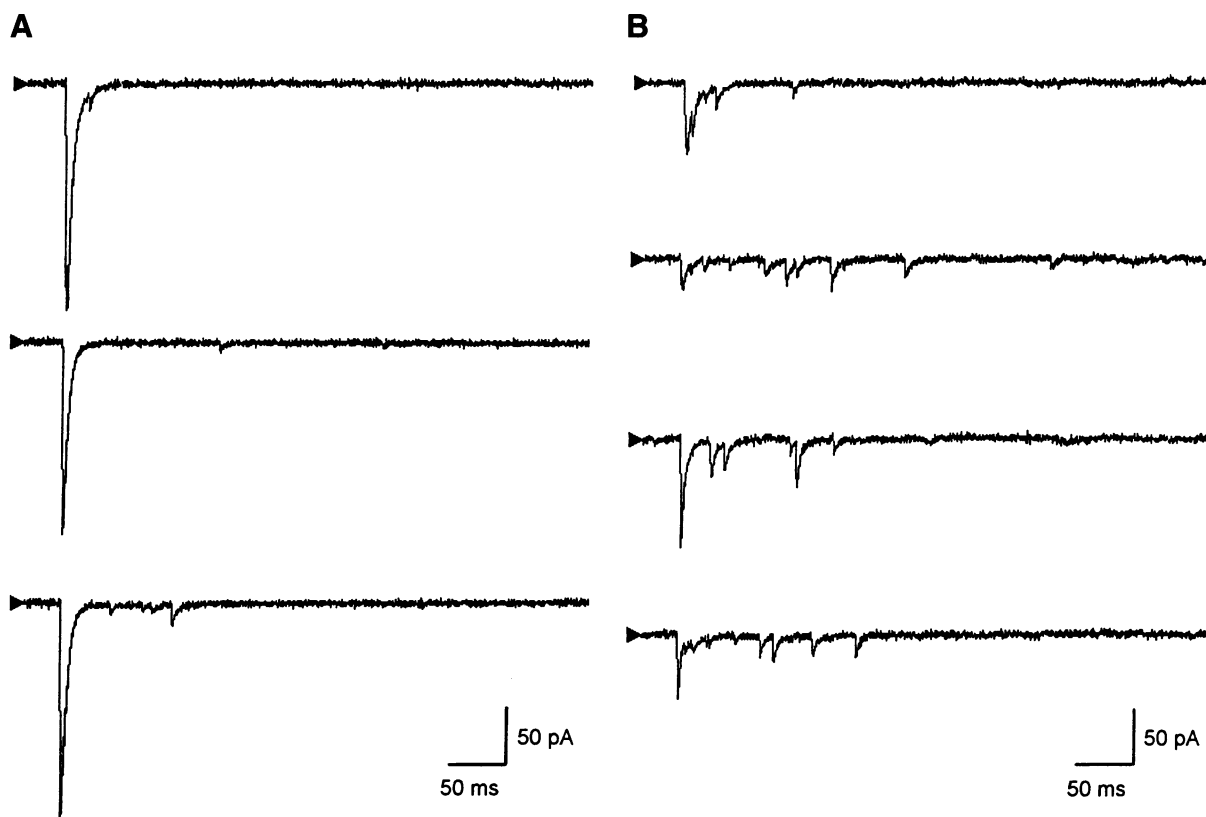


FIG. 2. Example traces of recordings carried out in 0.5 mM Mg^{2+} /10 mM Ca^{2+} (A) and in 0.5 mM Mg^{2+} /10 mM Sr^{2+} (B) from a cell pair (after 10 days in culture).

area was monitored by including a fluorescent dye in the perfusate, and subsequently the number of boutons present in the region of synaptic activation was counted by synapsin I immunofluorescence. In addition, the quantal size was estimated from the mean size of spontaneous synaptic currents.

Two components of transmitter release are present when roughly 16 boutons were stimulated on average in 0.5 mM Mg^{2+} and 10 mM Ca^{2+} (Fig. 4). These results confirm previous demonstrations of synaptic unreliability that used two different approaches involving minimal stimulation (12, 13) and an open channel blocker of postsynaptic glutamate receptors (14, 15). From the average quantal release rate for a single bouton, we can place an upper limit of 0.46 quanta released in the first 20 ms after the nerve impulse arrival at the presynaptic terminal under optimal release conditions (increased Ca^{2+} concentration and decreased Mg^{2+} concentration). Thus at most a single quantum is released only half the time for a given stimulus at an average hippocampal synapse.

Table 2. The effects of Sr^{2+} substitution on the magnitude of synaptic responses

Mg^{2+} , mM	Ca^{2+}/Sr^{2+}	n^*	% response in Sr^{2+} relative to Ca^{2+}	
			Fast component [†]	Slow component [†]
5	3	3	13 ± 5	122 ± 86
2	3	6	29 ± 7	260 ± 120
2	5	6	21 ± 6	210 ± 57
0.5	10	5	44 ± 8	330 ± 35

For each cell pair, 20 evoked responses in Ca^{2+} and in Sr^{2+} were averaged to obtain the release rate histograms for analysis.

*Number of cell pairs.

[†]Fast and slow components, *F* and *B*, respectively, are as defined in Fig. 1 legend.

DISCUSSION

We have provided evidence for two distinct components of transmitter release in hippocampal neurons: a fast, synchronous component of release whose efficacy is reduced in the presence of Sr^{2+} and a slower asynchronous component of release that is greatly facilitated by the Sr^{2+} substitution of external Ca^{2+} ; both components of synaptic responses conform to the standard cooperativity of transmitter release ($n \approx 4$) as predicted by the Dodge–Rahamimoff equation.

A central role played by Ca^{2+} in evoked synaptic transmission limits the most plausible explanations for the two components of release to the following: (i) the extent of Ca^{2+} -dependent release is limited by the decay of Ca^{2+} transient in the presynaptic terminal that displays two time constants, or (ii) the Ca^{2+} -dependent activation/inactivation of release machinery itself falls into two categories. The first scenario would imply the presence of at least two different Ca^{2+} buffering systems: a low-affinity buffer would define the fast component, and a slower acting second Ca^{2+} -clearance mechanism with a higher Ca^{2+} affinity would then account for the second component of release. In this case, the Sr^{2+} substitution experiments would be explained if we assume that the low-affinity Ca^{2+} buffer displays higher affinity toward Sr^{2+} , thus reducing the magnitude of the fast component. The second component is assumed not to clear Sr^{2+} as efficiently, thus raising the tail of the Sr^{2+} transient, which in turn facilitates the second component of release.

The second scheme would involve Ca^{2+} -sensitive molecules, which would divide the overall transmitter release into two processes with distinct properties. For example, a low-affinity Ca^{2+} sensor that assists release very effectively would promote the synchronous phase of release when the Ca^{2+} concentration in the presynaptic terminal is very high—that is, immediately following the stimulus. A high-affinity Ca^{2+} sensor that is less efficient in facilitating release would

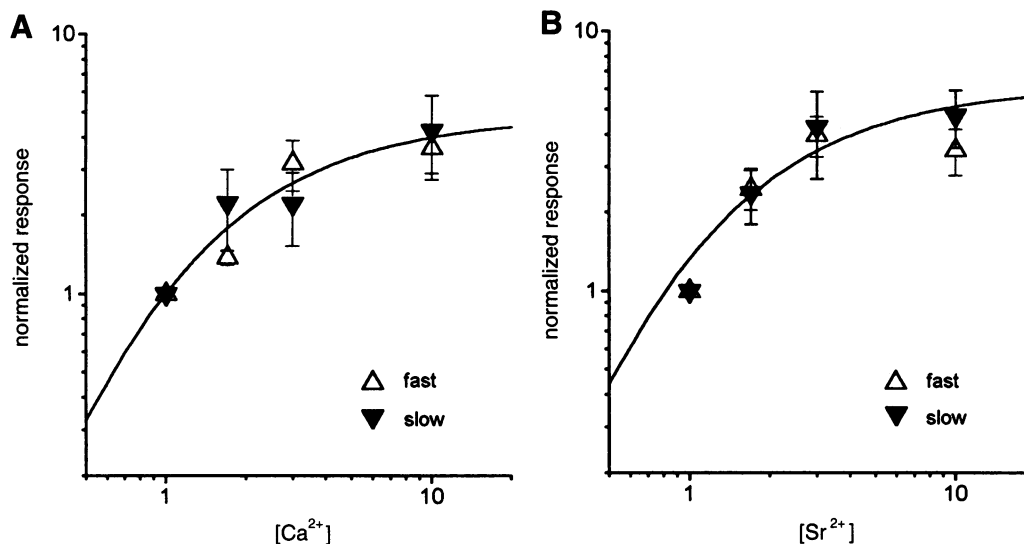


FIG. 3. Dependence of synaptic responses to extracellular Ca^{2+} or Sr^{2+} ion concentrations conform to the Dodge–Rahamimoff equation with a cooperativity of 4. The fast (Δ) and the slow (∇) components of synaptic responses are plotted against Ca^{2+} concentrations of 1 mM ($n = 11$), 1.7 mM ($n = 4$), 3 mM ($n = 7$), and 10 mM ($n = 4$) (A) or Sr^{2+} concentrations of 1 mM ($n = 10$), 1.7 mM ($n = 3$), 3 mM ($n = 4$), and 10 mM ($n = 5$) (B). Mg^{2+} concentration was kept constant at 0.5 mM. Responses to 1 mM and at least one additional Ca^{2+} or Sr^{2+} concentration were determined for each pair of cells, and the responses were normalized against the value obtained for 1 mM Ca^{2+} or Sr^{2+} . The fast and slow components are as defined in Fig. 1 legend. The error bars indicate \pm SEM. The points were fitted to the Dodge–Rahamimoff equation: $R(x) = [Wx/(1 + x/K_1 + 0.5/K_2)]^n$, where $n = 4$ and $x = \text{Ca}^{2+}$ or Sr^{2+} concentration (solid line). The parameters for optimal fit as shown were $W = 5.01$, $K_1 = 0.296$, and $K_2 = 0.812$ for Ca^{2+} and $W = 5.07$, $K_1 = 0.3116$, and $K_2 = 1.006$ for Sr^{2+} .

sustain asynchronous release during the period after the Ca^{2+} transient when there is persistent residual increase in the intraterminal Ca^{2+} concentration. In this model, Sr^{2+} would have differential effects on the overall release process facilitated by the two sensors: Sr^{2+} impedes the release assisted by the low-affinity sensor, whereas Sr^{2+} binding enhances the efficacy of the high-affinity sensor.

We favor the “two Ca^{2+} sensor” hypothesis, although we cannot exclude the other alternative. Molecular characterization of the synaptic vesicle-associated components has led to the identification of synaptotagmin as a possible molecule mediating Ca^{2+} -dependent transmitter release (16–22). Indeed we have recently demonstrated a specific role for

synaptotagmin I in the fast component of transmitter release in hippocampal neurons (8). Our two Ca^{2+} sensor hypothesis should provide a framework for further investigations. It would be of interest, for example, to examine the possible role of other members of the synaptotagmin family (23–25) as the second, high-affinity sensor that mediates asynchronous release.

APPENDIX

Three methods are available for estimating the rate of quantal release, each with its own advantages and disadvantages: direct counting of each quantum (26), measurement of the quantal latency distribution (1), and the synaptic current integration method frequently used in studies of synaptic transmission.

The purpose of this appendix is to provide an estimate of the range of validity for the method that we have used to determine the quantal release rate. Let $Q(t)$ represent the average mEPSC, so that the total current measured $I(t)$ at time t is given, for noninteracting quanta, by

$$I(t) = \int_0^\infty Q(t-x)r(x)dx,$$

where $r(t)$ is the release rate that we wish to measure. Since the quantal response is brief, we approximate Q by the series (27) $Q(t) = Q_0\delta(t) - Q_1\delta'(t) + \dots$, where $\delta(t)$ is the Dirac delta function and $\delta'(t)$ is its first derivative; Q_0 and Q_1 are given by $Q_0 = \int_0^\infty Q(t)dt$ and $Q_1 = \int_0^\infty tQ(t)dt$. Thus Q_0 is the average total charge transfer produced by a single quantum, and Q_1 is associated with characteristic time for the charge transfer. For a mEPSC approximated by an instantaneous rise and a single exponential decay, $Q_1 = Q_0\tau$, as can be seen by carrying out the integrals with decay time constant τ .

With the approximate representation of the quantal response, the measured current is seen to be

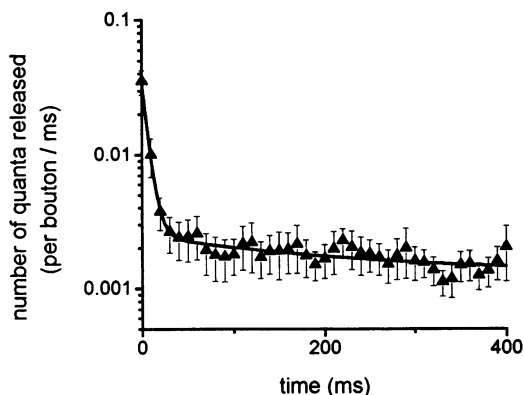


FIG. 4. Quantal release rate displays two components of decay. The average quantal release rate per bouton in 0.5 mM Mg^{2+} /10 mM Ca^{2+} ($n = 7$ cell pairs) was determined by employing a local microperfusion protocol (see *Materials and Methods*); the mean quantal charge was determined from mEPSCs between stimulation. The error bars indicate \pm SEM. The quantal release rate was fitted to the double-exponential equation described in Fig. 1 legend (solid line). Quantal release rate of the fast and slow components is 0.023 per bouton per ms and 0.0012 per bouton per ms (coefficient B), respectively, with associated decay time constants of 6.5 ms (a^{-1}) and 200 ms (b^{-1}). Other parameters are $A = 0.0333$ per bouton per ms and $C = 0.0013$ per bouton per ms.

$$I(t) = \int_0^{\infty} (Q_0 \delta(t-x) - Q_1 \delta'(t-x) + \dots) r(x) dx$$

$$= Q_0 r(t) + Q_1 \frac{dr(t)}{dt} + \dots$$

Thus, as long as the release rate is slowly varying on the time scale set by the decay time of Q , the higher order terms can be neglected, and the release rate is estimated by

$$r(t) \approx \frac{I(t)}{Q_0},$$

that is, by the measured synaptic current divided by the charge transferred by the response to a single quantum. The error can be estimated for the specific case of an exponentially decaying quantal response (time constant τ) and a release rate with the form $r(t) = e^{-t/T}$, with a decay time constant T . For this model case, the release rate is given, to first order, by

$$r(t) \approx \frac{I(t)}{Q_0} \left(1 - \frac{\tau}{T} \right).$$

This approximation is adequate for the slow, but not the fast, components of transmitter release.

We thank Dr. Thomas Südhof for the anti-synapsin I antibody. This work was supported by the Howard Hughes Medical Institute (C.F.S.) and National Institutes of Health Grant 5 RO1 NS 12961-17 (C.F.S.). Y.G. is supported by a Young Investigator Award from the National Alliance for Research on Schizophrenia and Depression.

1. Barrett, E. F. & Stevens, C. F. (1972) *J. Physiol.* **227**, 691-708.
2. Miledi, R. (1966) *Nature (London)* **212**, 1233-1234.
3. Meiri, U. & Rahamimoff, R. (1971) *J. Physiol.* **215**, 709-726.
4. Zengel, J. E. & Magleby, K. L. (1980) *J. Gen. Physiol.* **76**, 175-211.
5. Stevens, C. F. (1993) *Cell* **10**, 55-63.
6. Segal, M. M. & Furshpan, E. J. (1990) *J. Neurophysiol.* **64**, 1390-1399.
7. Bekkers, J. M. & Stevens, C. F. (1991) *Proc. Natl. Acad. Sci. USA* **88**, 7834-7838.
8. Geppert, M., Goda, Y., Hammer, R. E., Li, C., Rosahl, T. W., Stevens, C. F. & Südhof, T. C. (1994) *Cell*, in press.
9. Rosahl, T. W., Geppert, M., Spillane, D., Herz, J., Hammer, R. E., Malenka, R. C. & Südhof, T. C. (1993) *Cell* **75**, 661-670.
10. Forsythe, I. D. & Westbrook, G. L. (1988) *J. Physiol.* **396**, 515-533.
11. Dodge, F. A. & Rahamimoff, R. (1967) *J. Physiol.* **193**, 419-432.
12. Raastad, M., Storm, J. F. & Andersen, P. (1992) *Eur. J. Neurosci.* **4**, 113-117.
13. Allen, C. & Stevens, C. F. (1994) *Proc. Natl. Acad. Sci. USA* **91**, 10380-10383.
14. Rosenmund, C., Clements, J. D. & Westbrook, G. L. (1993) *Science* **262**, 754-757.
15. Hessler, N. A., Shirke, A. M. & Malinow, R. (1993) *Nature (London)* **366**, 569-572.
16. Brose, N., Petrenko, A. G., Südhof, T. C. & Jahn, R. (1992) *Science* **256**, 1021-1025.
17. Davletov, B. A. & Südhof, T. C. (1993) *J. Biol. Chem.* **268**, 26386-26390.
18. Bommert, K., Charlton, M. P., DeBello, W. M., Chin, G. J., Betz, H. & Augustine, G. J. (1993) *Nature (London)* **363**, 163-165.
19. Elferink, L. A., Peterson, M. R. & Scheller, R. H. (1993) *Cell* **72**, 153-159.
20. DiAntonio, A., Parfitt, K. D. & Schwartz, T. L. (1993) *Cell* **73**, 1281-1290.
21. Littleton, J. T., Stern, M., Schulze, K., Perin, M. & Bellen, H. J. (1993) *Cell* **74**, 1125-1134.
22. Nonet, M. L., Grundahl, K., Meyer, B. J. & Rand, J. B. (1993) *Cell* **73**, 1291-1305.
23. Geppert, M., Archer, B. T. & Südhof, T. C. (1991) *J. Biol. Chem.* **266**, 13548-13552.
24. Mizuta, M., Inagaki, N., Nemoto, Y., Matsukura, S., Takahashi, M. & Seino, S. (1994) *J. Biol. Chem.* **269**, 11675-11678.
25. Hilbush, B. S. & Morgan, J. I. (1994) *Proc. Natl. Acad. Sci. USA* **91**, 8195-8199.
26. Katz, B. & Miledi, R. (1965) *Proc. R. Soc. London B* **161**, 483-495.
27. Lindell, I. V. (1993) *Am. J. Phys.* **61**, 438-442.